Fractality in multiparticle production – a graph theoretical approach

P. Mali[1],* S. K. Manna[2], A. Mukhopadhyay[1], P. K. Haldar[3], and G. Singh[4]
[1]*Department of Physics, University of North Bengal, Siliguri 734013, India*
[2]*Department of Physics, Chakdaha College, Chakdaha, Nadia 741222, India*
[3]*Department of Physics, Dinhata College, Coochbehar 736115, India and*
[4]*Department of Computer and Information Science, SUNY at Fredonia, NY 14063, USA*

Time series analysis is a powerful method that can characterize data of any kind of sequential measurements. Recently the duality between time series and visibility graph (network) analysis has been established. Time series analysis in terms of visibility graph (VG) has emerged as a focal issue in nonlinear science and mathematics [1]. An ordinary VG is generated from a time series following the criterion: two arbitrary data points (t_a, y_a) and (t_b, y_b) in the time series have visibility and hence they constitute two nodes in the associated graph, if any other point (t_c, y_c) in between the previous two fulfills the condition

$$y_c < y_a + (y_b - y_a)\frac{t_c - t_a}{t_b - t_a}. \qquad (1)$$

On the other hand, a horizontal visibility graph (HVG) is mapped from the following visibility condition

$$y_a, y_b > y_c \quad \text{for all } t_a < t_c < t_b. \qquad (2)$$

The degree (k) of a node is defined as the number of edges (connections) that it has with other nodes. Obviously for a given time series the HVG is a subgraph of its associated VG. Here we report some results on the HVG analysis of the pseudorapidity (η) distribution of shower tracks coming out of ^{16}O+Ag/Br collisions at $E_{\rm lab}$ = 200A GeV. High multiplicity ^{16}O+Ag/Br events are chosen for by using a multiplicity cut $n_s > 100$. An event sample similar to the experimental one but five times larger in statistics is simulated by

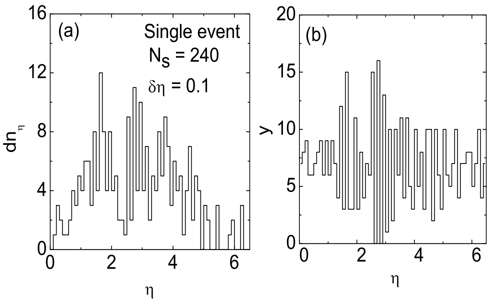

FIG. 1: (a) η distribution and (b) the modified distribution of one ^{16}O+Ag(Br) event.

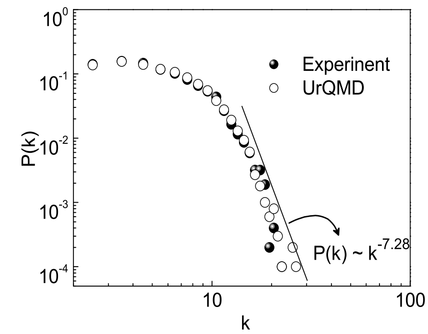

FIG. 2: Degree distribution of HVG for the modified distributions.

using the UrQMD code [3]. The experimental details are given in [2], while the simulation technique is outlined in [4]. The η-distribution of one experimental event with n_s = 240 is shown in FIG. 1(a), which exhibits rapid fluctuations around an Gaussian trend. Here dn_s is the number of shower tracks falling within a particular η-interval ($d\eta = 0.1$ here). To ensure that the overall shape of the distribution does not adversely affect the visibility between two nodes, the fluctuations are detrended by considering successive differences, $y_i = dn_s(\eta_{i+1}) - dn_s(\eta_i)$. The y_i values is then mapped to the positive plane and

*Electronic address: provashmali@gmail.com

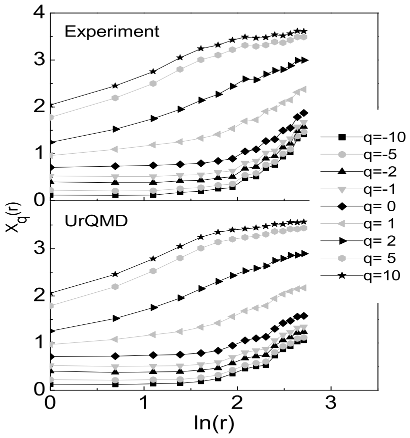

FIG. 3: Box size dependence of $X_r(q)$ where $X_q(r) = \ln \langle [M(r)]^{q-1} \rangle$ for $q \neq 1$ and $X_{q=1}(r) = \ln \langle [M(r)] \rangle$.

such a plot of y_i corresponding to the event of FIG. 1(a) is shown in FIG. 1(b), which is now approximately uniform where relative fluctuations are retained. On an event by event basis η-distributions so modified are now converted into corresponding HVG and an overall degree distribution $P(k)$ for the entire event sample is obtained, which is plotted in FIG. 2. It seems that both experimental and simulated data sets yield almost identical $P(k)$. The tail region of the degree distribution is fitted to a power-law: $P(k) \sim k^{-\lambda_p}$. The tail exponent λ_p (= 7.28 here), commonly known as the Power of Scale-freeness in Visibility Graph (PSVG), far exceeds the limit for a correlated (long range) time series. In the sandbox (SB) algorithm [5] the generalized fractal dimensions of a network are measured as,

$$D_{q\neq 1} = \lim_{r\to 0} \frac{\ln \langle [M(r)]^{q-1} \rangle}{\ln r} \left(\frac{1}{q-1} \right), \quad q \in R,$$
$$D_1 = \lim_{r\to 0} \frac{\ln \langle [M(r)] \rangle}{\ln r}, \qquad (3)$$

where $M(r)$ is the number of points in a sandbox of radius r, and the brackets $\langle \cdot \rangle$ stand for a statistical average of several sandboxes of same size, but chosen at random over the network. The mass exponents $\tau(q)$ and the singularity spectrum $f(\alpha_q)$ are calculated as $\tau(q) = (q-1)\, D_q$ and $f(\alpha) = q\alpha_q - \tau(q)$, where $\alpha = \partial\tau(q)/\partial q$ is the mass exponent. We apply the SB algorithm

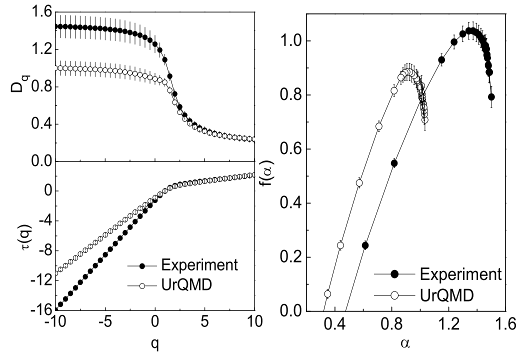

FIG. 4: Plots of the generalized fractal dimensions D_q, the mass exponents $\tau(q)$ and the spectral functions $f(\alpha_q)$.

to compute $\langle [M(r)]^{q-1} \rangle_{q\neq 1}$ and $\langle [M(r)] \rangle_{q=1}$ to characterize the observed fluctuations in terms of (multi)fractality. The event averaged $\langle [M(r)]^{q-1} \rangle_{q\neq 1}$ and $\langle [M(r)] \rangle_{q=1}$ values plotted against box size r are shown in FIG. 3. We perform linear regressions to estimate D_q in the region $7 \leq r \leq 15$. The order dependences of D_q and $\tau(q)$ are shown in FIG. 4(left), whereas the spectral functions are plotted in FIG. 4(right). All parameters indicate that multifractality is present both in the experiment and in the UrQMD simulated distributions. The degree of multifractality however, seems to be significantly larger in the experiment than in the simulation. Unlike the detrended and other popular methods [4, 6], where hardly any difference has been seen in the (multi)fractal nature of the experiment and UrQMD simulation, the graph theoretical approach adopted here seems to be a more effective tool to distinguish between the two.

References

[1] L. Lacasa *et al. Proc. Natl. Acad. Sci. U.S.A.* **105**, 4972 (2008).
[2] D. Chanda *et al., Phys. Rev.* **C 71**, 034904 (2005).
[3] S. A. Bass *et al., Prog. Part. Nucl. Phys.* **41**, 255 (1998).
[4] P. Mali *et al., Physica* **A 424**, 25 (2015).
[5] T. Tél *et al., Physica* **A 159**, 155 (1989).
[6] R.C. Hwa, Phys. Rev. **D 41**, 1456 (1990), F. Takagi, *Phys. Rev. Lett.* **72**, 32 (1994), P. Mali *et al., Physica* **A 450**, 323 (2016).